Multi-decadal ozone air quality and the role of temperature in Switzerland during summertime

Clara M. Nussbaumer[1], Colette L. Heald[1], Amanda M. Häne[1], and Christoph Hüglin[2]

[1]Institute for Atmospheric and Climate Science (IAC), ETH Zürich, 8092 Zürich, Switzerland
[2]Swiss Federal Laboratories for Materials Science and Technology (Empa), 8600 Dübendorf, Switzerland

Correspondence: Clara M. Nussbaumer (clara.nussbaumer@env.ethz.ch) and Colette L. Heald (colette.heald@env.ethz.ch)

Abstract. Tropospheric ozone (O_3) is a greenhouse gas and air pollutant. Despite efforts to control O_3 precursor emissions, O_3 levels frequently exceed the Swiss air quality standards. We present multi-decadal summertime measurements of O_3 and its precursors across Switzerland from 12 NABEL (Nationales Beobachtungsnetz für Luftfremdstoffe) stations, which are representative of traffic, (sub)urban, rural and background conditions. Average O_3 levels have decreased at rural and background

5   sites, remained constant at (sub)urban sites and increased under traffic conditions over the past two decades. Traffic, (sub)urban and rural sites exhibited a pronounced weekend effect at the beginning of the century, which has weakened over time and only persists under traffic conditions today, suggesting that O_3 formation is becoming more NO_x-sensitive. O_3 exhibits a strong dependence on temperature (dO_3/dT), which has weakened uniformly at all site types over time. At polluted sites, this effect could be associated with the decreasing influence of titration. While reductions of precursor levels have shifted the probabil-

10 ity of O_3 exceedances to higher temperatures, O_3 is still frequently exceeded on hot summer days and the number of days exceeding $30\,°C$ has tripled since 2000. Ozone formation has been suppressed due to the titration by NO in many locations in the past but is dominated by NO_x-sensitive O_3 chemistry in background, rural, and (sub)urban environments today. Ozone titration remains dominant under traffic conditions, where O_3 levels are currently increasing with NO_x and will likely increase for several years before emissions reductions will become effective.

1 Introduction

Tropospheric ozone (O_3) adversely impacts climate and human health as a greenhouse gas and air pollutant. In urban areas, it contributes to poor air quality increasing the risk of cardiovascular and respiratory diseases, and associated premature mortality (Nuvolone et al., 2018). A recent study by Wang et al. (2025b) estimated that approximately 94 % of the global population is chronically exposed to unhealthy levels of O_3 resulting in approximately 1.4 million premature deaths annually. In the European

20 Union, 70,000 deaths were attributed to O_3 exposure in 2022 as reported by the European Environmental Agency (2024). In light of these impacts, governmental air quality standards are implemented with the objective of improving public health. In Switzerland, this standard is set to a 1-hour average of $120\,\mu g\,m^{-3}$ ($\sim$60 ppbv) by the Swiss Ordinance of 16 December 1985 on Air Pollution Control (Luftreinhalte-Verordnung), which must not be exceeded more than once per year (Schweizerischer Bundesrat, 1985).
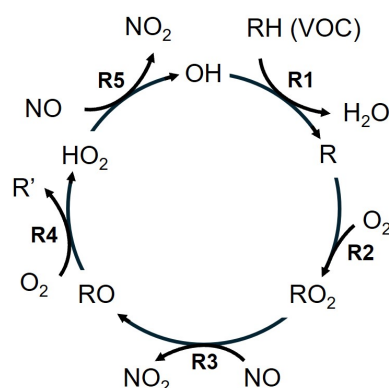
Figure 1. Catalytic O_3 formation cycle, highlighting the role of reactions (R1)-(R5).

25   O_3 is not emitted directly from a source but is photochemically formed from its precursors, which are nitrogen oxides (NO_x) and volatile organic compounds (VOCs). NO_x represents nitric oxide (NO) and nitrogen dioxide (NO_2) and is mainly emitted as NO from high-temperature processes, including combustion in vehicles, industrial activities and lightning, as well as NO_x from soils (Denman et al., 2007; Huang et al., 2017; Nault et al., 2017; Weng et al., 2020). VOCs are gaseous carbon-containing molecules of diverse origin, e.g., combustion, fuel evaporation, household and personal care products or vegetation (Guenther

30   et al., 2012; Sindelarova et al., 2014; McDonald et al., 2018; McDuffie et al., 2020). NO_x and VOCs form O_3 in the presence of sunlight. This catalytic O_3 formation cycle, as shown in Figure 1, is initiated by the oxidation of VOCs (here displayed as RH) by OH (R1), which produces peroxy radicals RO_2 in the presence of molecular oxygen O_2 (R2). RO_2 reacts with NO to form NO_2 and alkoxy radicals RO (R3), which further produce HO_2 with O_2 (R4). HO_2 oxidizes NO to NO_2 and at the same time regenerates the OH radical (R5). NO_2 subsequently forms NO and O_3 in the presence of sunlight via (R6a) and (R6b)

35   (Crutzen, 1988; Seinfeld and Pandis, 2016). In turn, NO and O_3 form NO_2 via (R7). NO_2 and O_3 interconvert on a time scale of minutes.

$$NO_2 + h\nu \rightarrow NO + O \tag{R6a}$$

$$O + O_2 + M \rightarrow O_3 + M \tag{R6b}$$

$$NO + O_3 \rightarrow NO_2 + O_2 \tag{R7}$$
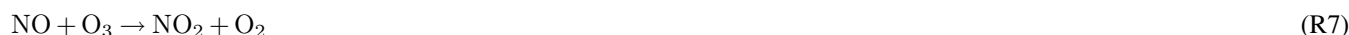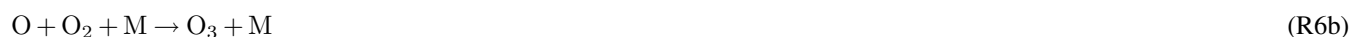
40   Close to NO emissions sources, for example in proximity to roads, O_3 is rapidly titrated to NO_2 via (R7). Therefore, NO_2 and O_3 are often considered as their sum: odd oxygen (O_x). Net O_3 production only occurs when NO_2 is generated from the

reaction of nitric oxide with peroxy radicals (RO_2 or HO_2) rather than O_3 as the latter is only a recycling mechanism. Various termination reactions of the catalytic cycle in Figure 1 make O_3 formation non-linear. These are mainly radical recombination, such as the self-reaction of the peroxy radical, as well as the reaction of NO_2 with OH forming nitric acid (HNO_3). As a

45   consequence, O_3 can either increase or decrease in response to precursor changes. For low NO_x environments, increasing NO_x leads to an acceleration of the catalytic O_3 formation cycle and O_3 production increases. This is referred to as NO_x-sensitive O_3 formation chemistry. For high NO_x in contrast, enhancements in NO_x lead to decreases in O_3 production due to the formation of nitric acid, which lowers the availability of OH radicals catalyzing the O_3 formation cycle. In this chemical environment, increases in VOCs lead to O_3 production enhancements and the chemistry is referred to as VOC-sensitive. O_3 formation peaks

50   between NO_x- and VOC-sensitive chemistry and the crossover occurs in a transitional regime (Pusede et al., 2015).

The non-linear formation chemistry of O_3 makes its control in urban environments challenging, as decreases in precursor emission, aimed at improving local air quality, can lead to O_3 increases instead when the formation chemistry is VOC-sensitive. In addition, close to emission sources the titration effect of O_3 via (R7) can dominate. O_3 changes with NO_x are then similar to those affected by VOC-sensitive chemistry, making it difficult to identify the required measures to achieve O_3 decreases. An

55   additional challenge is the lifetime of O_3, which is of the order of hours to days close to the surface, and of weeks to months in the free troposphere. Therefore, an exceedance of O_3 standards can result not only from local production, but also from long-range transport from outside the studied region (Cooper et al., 2011). Particularly remote sites are often dominated by the O_3 background rather than local formation. Derwent et al. (2015) reported an average of 16-24 ppbv of European surface O_3 originates from intercontinental transport in the Northern Extratropics. The contribution of transported O_3 to the total O_3

60   was found to exhibit a strong seasonal cycle with the largest impact in winter. In contrast, short-lived pollutants such as NO_x (lifetime of minutes to hours) are significantly easier to control with emission standards as reductions in local emissions directly translate to decreases in the local burden.

Various studies have investigated surface O_3 in urban environments. An important method for identifying the dominating formation sensitivity of O_3 is the weekend effect, which was originally suggested by Levitt and Chock (1976). Lower NO_x on

65   weekends due to less vehicle traffic, which is often observed in densely populated and polluted regions, causes O_3 to increase when chemistry is VOC-sensitive. This observation was reported by Fujita et al. (2003), Chinkin et al. (2003) and Pollack et al. (2012) for the Californian South Coast Air Basin (SoCAB), an area known for its poor air quality. More recent studies including Baidar et al. (2015), Nussbaumer and Cohen (2020), Perdigones et al. (2022) showed that SoCAB O_3 chemistry was transitioning and approaching NO_x sensitivity in recent years with lower O_3 on weekends compared to weekdays as an

70   outcome of successful emission reductions. While O_3 increases on weekends are often an indication for VOC-sensitive O_3 chemistry, decreased O_3 titration on weekends (via (R7)) due to less NO can also lead to higher weekend O_3, as shown by Murphy et al. (2007) close to Sacramento (US). In that case, the reaction of NO with O_3 outweighs the photolysis of NO_2, and the net loss of O_3 (k*[NO]*[O_3]-j(NO_2)*[NO_2]) proceeds faster than the reactions shown in Figure 1. Geddes et al. (2009) reported unchanged O_3 levels in Toronto, Canada, between 2000 and 2007 despite significant precursor reductions, where

75   lowered O_3 production was countered by decreased O_3 titration.

A number of studies have investigated O_3 trends across Europe over the past decades, many of which reported increases in surface O_3 despite precursor reductions, particularly in polluted regions (Yan et al., 2018; Boleti et al., 2020; Adame et al., 2022; Massagué et al., 2024; Wang et al., 2025a). These studies highlight the continued need to monitor O_3 and its formation processes in Europe. Fewer studies have focused on O_3 in Switzerland. Ordoñez et al. (2005) investigated O_3 in Switzerland
80   between 1992 and 2002 and found O_3 titration and dry deposition to be the prevailing processes during winter, while summertime O_3 was dominated by O_3 production. Aksoyoglu et al. (2014) reported increases in average surface O_3 at all sites in Switzerland between 1990 and 2005 based on observations and modeling. These increases were attributed to the reduced impact of titration at polluted sites and to changes in background O_3 at the remaining sites. In contrast to average O_3, peak O_3 was found to decrease at rural sites. Boleti et al. (2018) analyzed changes in surface O_3 in Switzerland between 1990 and
85   2014 and found that O_3 was increasing at the majority of the 21 investigated stations until the mid 2000s, but was decreasing afterwards. The trend reversal occurred earlier for sites further away from NO_x emissions sources and later for sites impacted by traffic. Boleti et al. (2019) reported continuous decreases in peak O_3 in Switzerland over the same time period.

O_3 exhibits a strong dependence on temperature, as highlighted by various studies in the U.S., Europe and Asia (Pusede et al. (2015), Coates et al. (2016), Porter and Heald (2019), Nussbaumer and Cohen (2020), Wu et al. (2024), Chang et al. (2025) and
90   Qin et al. (2025)). Explanations for this correlation are numerous and include meteorological reasons, such as stagnation and humidity, as well as an enhanced abundance of precursors, e.g. temperature-dependent VOC emissions, soil NO_x emissions or PAN (peroxy acetyl nitrate) decomposition (Porter and Heald, 2019). Li et al. (2025) reported a 50 % decrease in the temperature dependence of summertime O_3 in the U.S. between 1990 and 2021 as a combined outcome of meteorological changes and anthropogenic NO_x reductions, the latter reducing the O_3 impact of temperature-dependent biogenic VOCs, dry
95   deposition and PAN decomposition (decrease in the O_3-T sensitivity). This was found to outweigh increases in the O_3-T sensitivity by soil-NO_x emissions under anthropogenic NO_x reductions.

In this study, we investigate summertime O_3 in Switzerland between 2000 and 2024 based on 12 different ground-based measurement sites. We present decadal trends for O_3, its precursors and exceedance probabilities of current air quality standards under traffic, (sub)urban, rural and background conditions, as well as day-of-week patterns and the correlation with
100   temperature. This study provides valuable insights into the photochemical mechanisms that control O_3 levels in Switzerland and the required measures to minimize its abundance.

2 Methods

2.1 NABEL network

We use surface observations from the NABEL (Nationales Beobachtungsnetz für Luftfremdstoffe) network, which provides
105   long-term measurements of trace gases and meteorology at 16 different sites in Switzerland (Hüglin et al., 2024). The network is maintained and operated by the Federal Office of the Environment (FOEN) and the Swiss Federal Laboratories for Materials Science and Technology (Empa). The meteorological data are provided by NABEL (stations BER, LAU, ZUE, DUE, DAV, RIG) and MeteoSwiss (stations BAS, CHA, LUG, MAG, PAY, TAE). For this analysis, we chose 12 sites representative
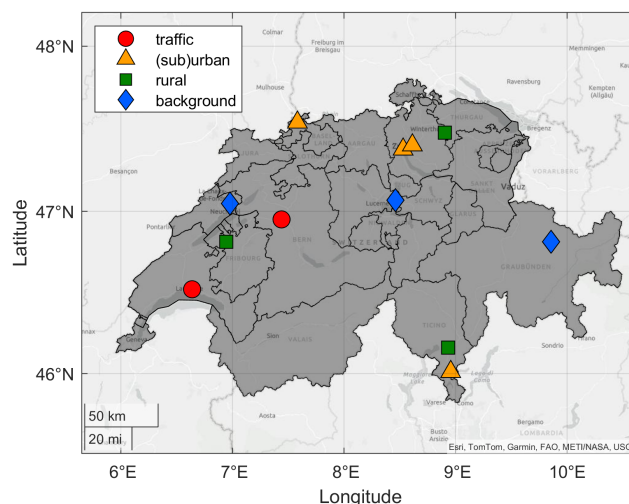
Figure 2. Location of the NABEL sites used in this study. ©Map Data: swisstopo (Federal Office of Topography swisstopo, 2024)

of traffic (Bern-Bollwerk BER and Lausanne-César-Roux LAU), (sub)urban (Zürich-Kaserne ZUE, Dübendorf-Empa DUE,
110 Basel-Binningen BAS and Lugano-Universita LUG), rural (Magadino-Cadenazzo MAG, Payerne PAY and Tänikon TAE) and
background (Chaumont CHA, Davos-Seehornwald DAV and Rigi-Seebodenalp RIG) conditions with a record of O_3 since the
year 2000. We define the background as rural sites between 1000 m and 2000 m altitude (excluding sites at higher altitudes
that predominantly sample the free troposphere). The sites RIG and CHA are located at the slope and the ridge of mountains,
respectively, and are therefore impacted by the nocturnal residual layer during the night and in the morning hours. Figure
115 2 shows a map with the location of the NABEL sites used here. We use trace gas observations of NO, NO_2 and O_3. At the
majority of the stations, NO and NO_2 are measured via chemiluminescence with a molybdenum converter (employment of three
different instrument types: APNA 370 NO_x monitor (HORIBA), 42i TL / 42iQ TL NO_x Analyzer (Thermo Fisher Scientific)
and T200 NO_x Analyzer (Teledyne API)). O_3 is measured via UV-absorption (49i ozone analyzer, Thermo Fisher Scientific).
The measurement uncertainties of NO, NO_2 and O_3 comply with the requirements for regulatory measurements and are in the
120 range of the limit values $< 10\,\%$ (Empa and BAFU, 2024). The observed variability is dominated by the atmospheric conditions
and the influence of local sources rather than the instrumental uncertainty. We further use temperature, pressure and solar
radiation measurements, which are provided by Empa and BAFU at DAV, DUE, HAE, LAU, RIG, ZUE and by MeteoSwiss at
BAS, CHA, LUG, MAG, PAY, TAE. Further details regarding the location of the NABEL sites and the measurement methods
can be found in the NABEL technical report (Empa and BAFU, 2024). We do not include measurements of volatile organic
125 compounds in this study due to limited spatial and temporal availability.

2.2 Data Processing

Unhealthy levels of O_3 mostly occur in the summer months and we therefore focus this analysis on the months of April to
August. We use hourly values between 09:00 and 18:00 local time (UTC+2), which we refer to as daytime in the following.

Throughout the months of interest, these hours occur at least two hours after local sunrise and two hours before local sunset,
130 which we chose to minimize the substantial impact of the diurnal variation in the boundary layer height. For some analyses, we
have separated data into weekdays (Monday to Friday) and weekends (Saturday and Sunday). We further perform temperature-
dependent analyses and define a low (10-20 °C), medium (20-30 °C) and high ($\geq$ 30 °C) temperature range. For investigating
the exceedance probability of O_3 and O_x, we follow the air quality standards of the Swiss Ordinance of 16 December 1985
on Air Pollution Control (Luftreinhalte-Verordnung), which states that the 1-hour average values must not exceed $120 \mu g\, m^{-3}$
135 more than once per year (Schweizerischer Bundesrat, 1985). At all stations, we consider O_3 and O_x hourly values above
60 ppbv to be in exceedance of this standard. The exceedance probability (EP) is defined as the percentage of hours during
daytime from April to August with O_3 (O_3 EP) or O_x (O_x EP) exceeding 60 ppbv. The observational frequency at the NABEL
sites is highly consistent over time, which we show in Figure S1 of the Supplement for O_3, NO_x and temperature measurements.
At all stations, the data completeness exceeds 90 % for hourly measurements in each year.

3 Results and Discussions

3.1 Decadal Summertime Trends of Trace Gases

Figure 3 shows the decadal changes of summertime (a) NO_x, (b) O_3, (c) O_x and (d) the share of O_3 in O_x at traffic (red),
(sub)urban (orange), rural (green) and background (blue) sites between 2000 and 2024. The relative change between the begin-
ning and the end of the record is shown in the boxes in the top right corners. Solid boxes represent significant (p-value $\leq$ 0.05)
145 and dashed boxes represent insignificant (p-value > 0.05) trends. We show the $1\,\sigma$ standard deviation of the averaging in Figure
S2 of the Supplement, which highlights the atmospheric variability and ranges between 25 % for background O_x and 95 % for
urban NO_x.

    NO_x has decreased at all sites with a similar relative magnitude over the past two decades. All trends are significant. In
2000, average NO_x was around 60 ppbv at the traffic sites and has decreased to 20 ppbv today (-1.64 ppbv year^{-1}, R^2=0.93).
150 It should be noted, that the decrease plateaued between 2009 and 2017, and then continued to the present day. This plateau
is only pronounced at traffic sites, which could point towards the role of on-road emissions, and coincides with the time of
the disclosure of the Dieselgate scandal in September 2015. Grange et al. (2020) found a reduction in NO_x emissions by
up to 36 % from affected diesel vehicles as an outcome of hard- or software updates in the United Kingdom in the years
following 2015. Further research is required to determine to what degree emissions from the diesel fleet could have affected
155 the observed plateau in NO_x levels in Switzerland and the subsequent decline in the late 2010s. Average NO_x at (sub)urban
sites declined by around 2/3 (-0.48 ppbv year^{-1}, R^2=0.97) and halved at rural (-0.17 ppbv year^{-1}, R^2=0.97) and background
(-0.09 ppbv year^{-1}, R^2=0.83) sites. These NO_x reductions highlight the successful anthropogenic emission control in response
to legislative restrictions over the past decades and are ongoing. The extent of NO_x reductions is slightly smaller at rural and
background compared to traffic and (sub)urban sites ($\sim$ 1/2 vs $\sim$ 2/3), which is consistent with larger relative contributions
160 from natural NO_x emissions at more remote sites. At all sites, both NO and NO_2 have declined, as shown in Figure S3 of the
Supplement. At traffic sites, NO has declined faster than NO_2 (78 vs 53 %) and the ratio between NO and NO_2 has decreased
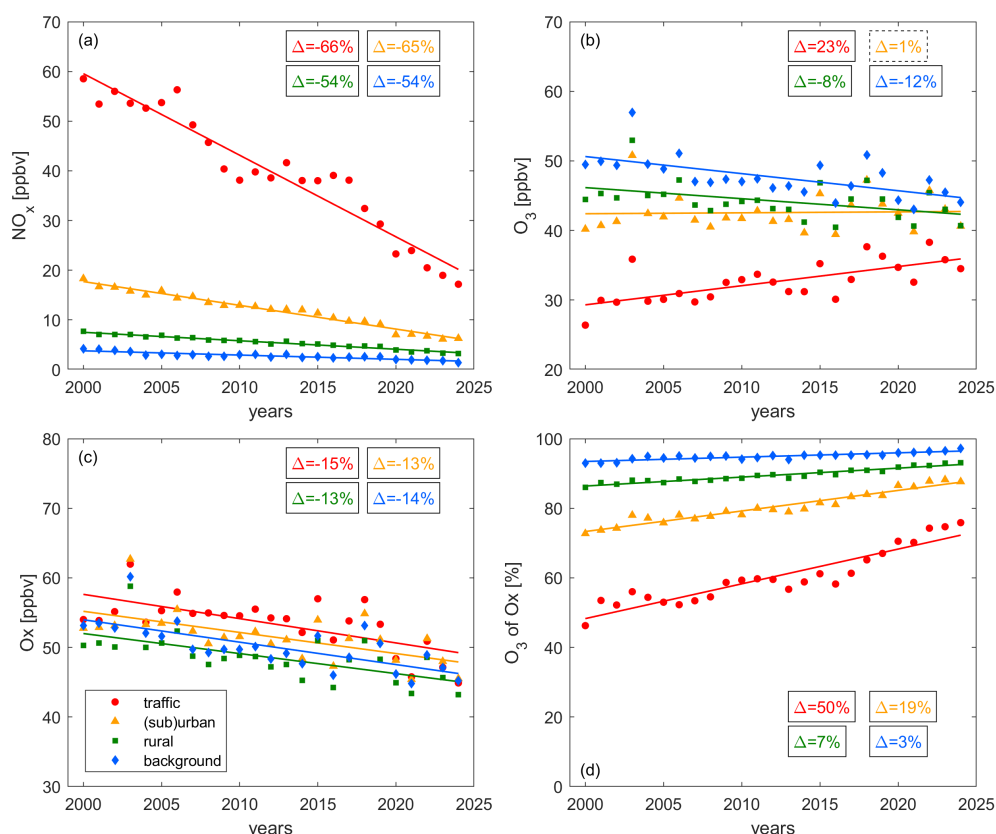
Figure 3. Decadal trends of (a) NO_x, (b) O_3, (c) O_x and (d) the share of O_3 in O_x at traffic (red), (sub)urban (orange), rural (green) and background (blue) sites. The markers show the yearly averages and the lines represent their associated linear fits. The boxes show the relative change of the trace gas levels between 2000 and 2024, whereby solid lines denote significant (p-value ≤ 0.05) and dashed lines insignificant (p-value > 0.05) trends.

from 1.1 to 0.6 over time as shown in Figure S3(c). The ratio declined faster before 2010 (from 1.1 to 0.7), with a more modest decline to present day (from 0.7 to 0.6). The majority of NO_x is emitted as NO and therefore, close to major sources, such as busy roads, the ratio of NO to NO_2 is expected to be higher compared to more remote areas. The observed decline in

165    $NO:NO_2$ over time is in line with findings from Hüglin and Rohrbach (2022), who investigated NO and NO_2 levels in Zürich (Switzerland), and could be an indication that NO emissions control has been more effective than NO_2 reductions or represent the increasing share of diesel vehicles on roads, with a higher share of NO_2 in NO_x emissions compared to gasoline cars. Empa (2024) reported an increase in overall tailpipe NO_2 emissions in Switzerland from 3,737 t year^{-1} in 2000 to 5,862 t year^{-1} in 2020 (peak in 2015 with 10,174 t year^{-1}), while NO_x emissions declined from 58,331 t year^{-1} in 2000 to 26,864 t year^{-1} in

170   2020. The increase in NO_2 emissions was entirely associated with diesel vehicles, partially offset by a decline in NO_2 emissions from gasoline engines. Grange et al. (2017) reported increases in the NO_2/NO_x ratio at European roadsides between 1995 and 2009 and a small decrease between 2010 and 2015. Potential explanations include the improvements of the exhaust after-

treatment technologies with subsequent Euro standards, both in light- and heavy duty vehicles, which lead to NO_x reductions with NO_2/NO_x emission ratios initially rising and then stabilizing and falling again from 2019 onward. The observed turnover
175　coincides with the change in rate, which we observe in 2010 for traffic sites in Switzerland.

Figure 3(b) shows the decadal changes of O_3. At the traffic sites, O_3 has increased by 0.28 ppbv year^{-1} (R^2=0.49) between 2000 and 2024. This increase occurred despite strong decreases in NO_x and can be explained by either a VOC-sensitive O_3 formation chemistry or the dominance of titration, with NO decreases "releasing" O_3. (Sub)urban O_3 does not show any trend over time with levels of around 40 to 45 ppbv, while rural O_3 has decreased by 0.16 ppbv year^{-1} since 2000 (R^2=0.20). The
180　strongest decrease over time can be observed in background O_3 by 0.25 ppbv year^{-1} (R^2=0.39). Overall, O_3 close to traffic emissions shows the lowest values, followed by (sub)urban and rural O_3. Background O_3 levels are highest, but the gap to traffic O_3 has diminished over time from an average of 20 ppbv in 2000 to 10 ppbv today.

Figure 3(c) shows O_x trends since 2000, which are decreasing at all sites with similar rates around 0.3 ppbv year^{-1} (R$^2 \sim 0.4$). While O_3 values show strong differences between the individual locations, O_x levels are more similar (around
185　50 ppbv today) highlighting the importance of partitioning between NO_2 and O_3. We would expect to see higher O_x for less remote locations due to stronger pollution, which can be observed for rural, followed by (sub)urban and traffic sites. In contrast, background O_x is higher than (sub)urban O_x. A potential explanation could be the impact of air masses entrained from the nighttime residual layer (with elevated O_3), coupled with the reduced effectiveness of loss processes such as deposition, titration or other nighttime chemical losses. An additional contribution could be the intrusion of free tropospheric air with higher
190　O_3 levels due to the elevation of the background sites (> 1000 m). O_x decreases over time at all sites despite the increase of O_3 at traffic sites due to the dominance of NO_2 reductions.

Figure 3(d) shows the changes in the share of O_3 in O_x over time, which increased at all sites. The increase is strongest for the most polluted sites and almost negligible for background conditions. At traffic sites, O_x consisted of 50 % O_3 and 50 % NO_2 at the beginning of the record, and the share of O_3 increased to around 75 % today. This suggests that the role of
195　titration has diminished over the past two decades and aligns with the observations of strong NO_2 decreases and O_3 increases. At (sub)urban sites the share of O_3 in O_x has increased from 75 to 90 % and at rural sites from 85 to 95 %. O_x at background sites is almost equal to O_3, which shows that titration is negligible.

Boleti et al. (2018) investigated trace gas trends at the NABEL sites between 1990 and 2014 and reported a reversal of increasing O_3 trends at certain "breakpoint" years. These breakpoints occurred earlier for more remote and later for more
200　polluted sites. They found a reversal of the trends at sites, which we categorize as rural and background, in the early 2000s. This is in line with our findings of decreasing O_3 trends under these conditions from 2000 onward. Boleti et al. (2018) further reported breakpoints for (sub)urban and traffic sites in the late 2000s and early 2010s, respectively. We observe a small decline at these sites between 2012 and 2014. However, this temporary reduction is a modest deviation from an overall increasing trend (during a short plateau in NO_x levels), which continues beyond the end of the study period of Boleti et al. (2018). Differences
205　between this study and Boleti et al. (2018) could additionally arise as the latter investigated meteorology-adjusted values of O_3 whereas we use direct observations.
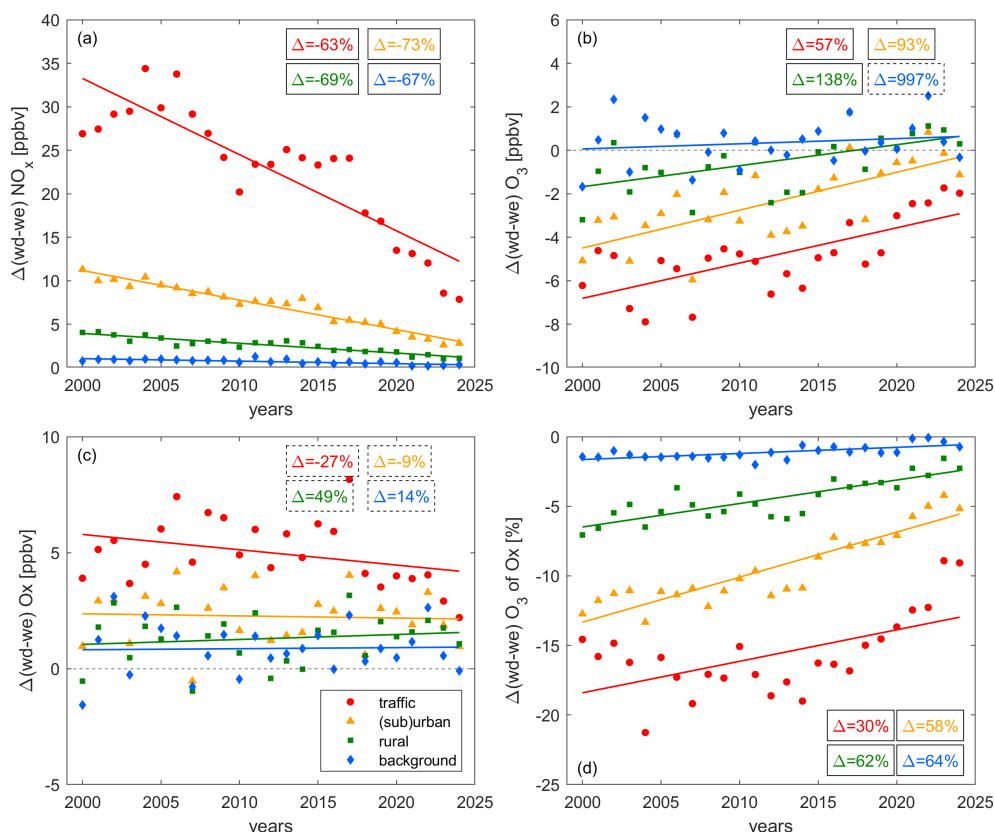
8

Figure 4. Decadal trends of the difference in weekday and weekend levels of (a) NO_x, (b) O_3, (c) O_x and (d) the share of O_3 in O_x at traffic (red), (sub)urban (orange), rural (green) and background (blue) sites. The markers show the yearly averages and the lines represent their associated linear fits. The boxes show the relative change of the trace gas levels between 2000 and 2024, whereby solid lines denote significant (p-value ≤ 0.05) and dashed lines insignificant (p-value > 0.05) trends.

3.2 Weekend Effect

Figure 4 shows the absolute differences between weekend and weekday levels of (a) NO_x, (b) O_3, (c) O_x and (d) the share of O_3 in O_x at traffic (red), (sub)urban (orange), rural (green) and background (blue) sites. Positive values indicate higher weekday and negative values higher weekend levels. Weekday NO_x is higher than weekend NO_x at all sites with the largest difference for traffic sites and diminishing differences with increasingly remote conditions. This is likely caused by strong day-of-week patterns in on-road vehicle emissions with commuter and freight traffic on weekdays, which is more pronounced in city centers. The background sites are not located in proximity to any roads. However, the lifetime of NO_x is on the order of a few hours to a day and the decline in NO_x at the background sites could reflect the decline in transported NO_x from nearby sources. The absolute weekend-weekday difference decreased significantly at all sites by around 2/3 between 2000 and 2024. However, the relative difference remained constant over time at the traffic sites (Figure S4). This suggests that the fleet

9

composition at the measured sites does not depend on the day of the week or that emission reductions have been consistent across different vehicle types. Weekday reductions at (sub)urban, rural and background sites have been more efficient than weekend reductions leading to an increase in the relative difference over time by 25 % (R^2=0.52), 25 % (R^2=0.43) and 12 %

220   (R^2=0.17), respectively (Figure S4). This could indicate that the fleet composition shows a different behavior than that observed for traffic sites or that different source types with day-of-week patterns are important at these sites, such as emissions from industrial activities. Further research is needed to understand these site-dependent magnitudes in NO_x reduction on weekdays vs weekends.

Figure 4 (b) presents the weekend-weekday changes of O_3 over time. The background sites do not show a pronounced

225   difference between weekdays and weekends, which is expected due to a small weekend-weekday difference in background NO_x levels. All other sites show a pronounced weekend-O_3 effect at the beginning of the record, which has decreased over time. Δ(wd-we) O_3 at traffic sites decreased from 7 ppbv in 2000 to around 2 ppbv today. (Sub)urban and rural Δ(wd-we) O_3 were 4 and 2 ppbv, respectively, in 2000. The difference in weekday and weekend O_3 is small at these (sub)urban and rural sites today. It is difficult to determine the precise timing of the reversal of the weekend effect, however, weekday O_3 has been higher

230   than weekend O_3 at rural stations continuously since 2019, while it has been mostly lower at (sub)urban sites. Higher weekday than weekend O_3 for higher weekday than weekend NO_x indicates dominating NO_x-sensitive chemistry. The observations therefore suggest that NO_x-sensitive chemistry has been dominant at background sites since the beginning of the record and that (sub)urban and rural sites are likely currently transitioning (or have recently transitioned) to NO_x-sensitive O_3 formation. Traffic sites are dominated by titration or VOC-sensitive O_3 formation, either of which could explain higher weekend than

235   weekday levels of O_3 as a result of lower weekend than weekday NO_x.

Figure 4 (c) shows that all sites are characterized by higher O_x on weekdays compared to weekends. For sites with a negligible impact of titration we expect the same weekend effect of O_3 and O_x (Murphy et al., 2007; Pusede and Cohen, 2012). This can be observed for background conditions, as well as rural sites in recent years and suggests dominating NO_x-sensitive O_3 formation. In contrast, for rural and (sub)urban sites at the beginning of the record as well as for traffic sites for

240   the entire period, O_3 has shown a distinct weekend effect with higher values on weekends, while O_x values have been higher on weekdays. This is suggestive of a sizeable impact of titration at rural and (sub)urban sites in the early 2000s and at traffic sites up to today, whereby a decrease of NO emissions on weekends shifts the equilibrium between NO_2 and O_3 towards O_3. No significant trend over time can be observed for the O_x weekend-weekday difference at any site.

In Figure 4 (d), we present the weekend-weekday difference of the share of O_3 in O_x. While no significant difference can

245   be observed for background sites, all other sites exhibit a higher share of O_3 on weekends. This weekend effect is strongest for traffic, followed by (sub)urban and rural sites, which aligns with the findings for the weekend effect of NO_2 and O_3 and emphasizes that titration still plays a major role at traffic sites today.
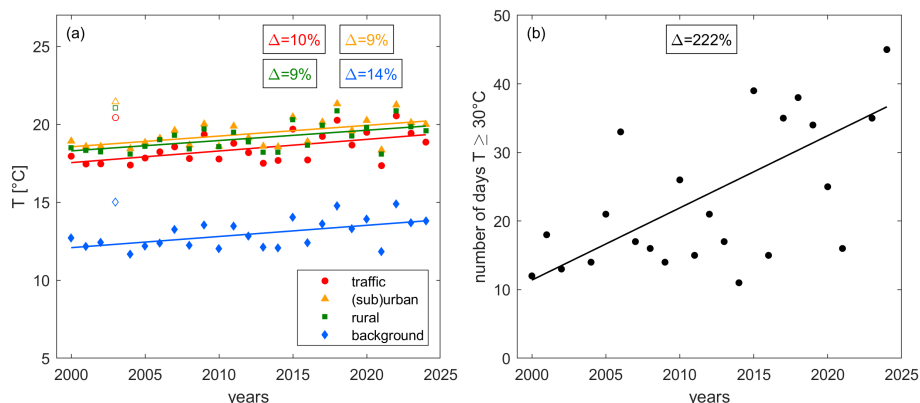
Figure 5. Decadal trends of (a) average April-August daytime temperature at traffic (red), (sub)urban (orange), rural (green) and background (blue) sites and (b) the number of days above $30\,^{\circ}C$ (accounting for the maximum temperature at traffic, (sub)urban and rural stations combined). Boxes show the relative change between 2000 and 2024. Solid lines denote significant (p-value ≤ 0.05) and dashed lines insignificant (p-value > 0.05) trends.

3.3 The Effect of Temperature

3.3.1 Decadal Changes in Temperature

250 Figure 5 shows (a) the trend of average summer daytime temperature over time and (b) the changes in high temperature days, defined as the number of days between April and August where temperatures $30\,^{\circ}C$ for at least one hour. We have combined rural, (sub)urban and traffic sites in panel (b). The background sites are located at higher elevation and therefore show lower temperatures and a negligible number of exceedances. For the trend analysis we exclude the year 2003, which was a severe heatwave year and showed a temperature anomaly of more than $5\,^{\circ}C$ in Switzerland (Black et al., 2004; Schär et al., 2004).

255 We show these data points in Figure 5(a) as open symbols. An increase in average temperature by $1.5\,^{\circ}C$ is observed at all sites since the beginning of the century. This in line with the current literature reporting rapid surface temperature increases in Europe since the 1990s (Dong et al., 2017; Twardosz et al., 2021). Twardosz et al. (2021) reported a summer time warming of $0.070\text{-}0.075\,^{\circ}C\,\text{year}^{-1}$ in Switzerland between 1985 and 2020. The April to August average temperature was $13.8\,^{\circ}C$ at background sites and $19.2\,^{\circ}C$ at the remaining sites in 2024. The $1\,\sigma$ standard deviation of the averaging represents the inter-

260 annual variability is of the order of $50\,\%$ for the background sites and $30\,\%$ for the remaining sites. The number of days with a temperature exceeding $30\,^{\circ}C$ has increased more than 3-fold since 2000, when only around $10\,\text{days}$ ($\sim 7\,\%$ of all days) exhibited high temperatures, compared to $35\,\text{days}$ today (almost 1/4 of all days).

3.3.2 Relationship of Trace Gases and Temperature

Figure 6 presents the relationship between (a) NO_x, (b) O_3, (c) O_x and (d) the share of O_3 in O_x with temperature, which

265 all exhibit strong correlations. We focus on data points below 10 and above $35\,^{\circ}C$ when calculating correlations. We show
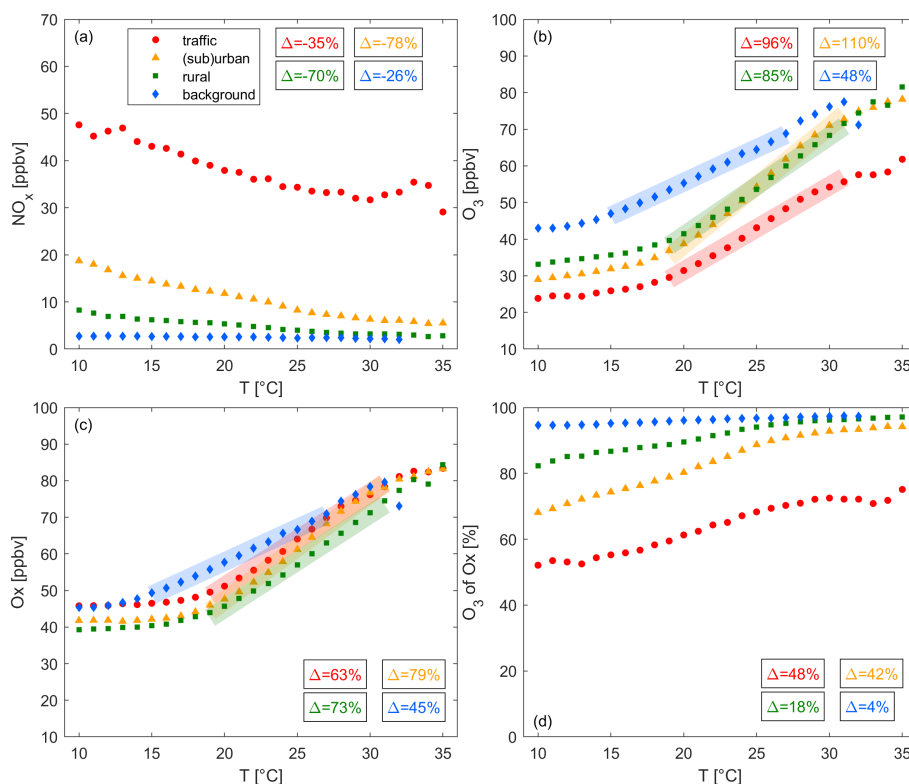
11

Figure 6. Changes of (a) NO_x, (b) O_3, (c) O_x and (d) the share of O_3 in O_x with temperature at traffic (red), (sub)urban (orange), rural (green) and background (blue) sites. The markers show the averages for each temperature bin. The boxes show the relative change of the trace gas levels for (a) and (d) between 2000 and 2024 and for (b) and (c) in the highlighted sections, whereby solid lines denote significant (p-value ≤ 0.05) and dashed lines insignificant (p-value > 0.05) trends.

the $1\,\sigma$ standard deviation of the averaging in Figure S5 of the Supplement. NO_x levels decrease at all sites with increasing temperatures, while O_3, O_x and the share of O_3 in O_x show a strong positive correlation with temperature.

The NO_x temperature anti-correlation is strongest for polluted sites and negligible for background sites. At traffic sites, NO_x mixing ratios decrease at a rate of 0.65 ppbv $°C^{-1}$. A slightly smaller decline of 0.54 ppbv $°C^{-1}$ can be observed for (sub)urban sites, followed by a decrease of 0.21 ppbv $°C^{-1}$ for rural sites. These observations suggest that the NO_x temperature correlation is linked to on-road NO_x emissions and is weaker for remote sites with a larger share of natural NO_x sources, such as soil NO_x, which is expected to increase with temperature (Oikawa et al., 2015). Light-duty diesel vehicles, particularly prior to the Euro-6 standard, show a strong anti-correlation of NO_x emissions and temperature. Grange et al. (2019) reported a decrease of NO_x emissions by a factor of 3 for pre Euro-6 passenger cars and light duty vehicles between 0 and 25°C. In Switzerland, the majority (> 90 %) of tailpipe NO_x is emitted from passenger cars, light duty vehicles and heavy duty vehicles (Empa, 2024). We are focusing on emissions within town limits. In 2020, passenger vehicles contributed 72 % of overall in-town NO_x vehicle emissions in Switzerland, followed by light-duty vehicles with 12 % and heavy duty vehicles with 8 %. 86 % of passenger

car NO_x emissions were attributed to diesel vehicles and close to 100 % of light and heavy duty vehicles were diesel-fueled. Therefore, overall 82 % of tailpipe NO_x was emitted by diesel vehicles in 2020. 36 % of passenger cars, 21 % of light duty

280 and 37 % of heavy duty vehicles on Swiss roads complied with the Euro-6 standard while most vehicles types were older (pre Euro-6) (Empa, 2024). Assuming an even distribution of gasoline and diesel vehicles on all street categories (in-town, out-of-town and highway), the share of temperature-dependent NO_x emissions was 49 % for passenger cars and light duty vehicles in 2020 and 54 % under the assumption that NO_x emissions from heavy duty vehicles exhibit a similar temperature dependence to those reported in (Grange et al., 2019). At traffic sites, NO_x mixing ratios decrease from 50 to 30 ppbv between 10 and

285 35 °C. Assuming the share of temperature-dependent NO_x emissions is representative of the middle of that temperature range (36 ppbv at 22 °C), on-road vehicles are the only source of NO_x at traffic sites, emissions relate linearly to mixing ratios and the temperature-dependence reported in (Grange et al., 2019) is similar between 10 and 35 °C, NO_x mixing ratios would decrease from 45 to 27 ppbv over this temperature-range. We conclude that the temperature dependence of NO_x emissions from diesel vehicles can plausibly explain the magnitude of the observed overall NO_x-temperature correlation. In 2010, the share of NO_x

290 emissions from diesel passenger cars was lower (61 %), however all on-road vehicles were pre Euro-6, leading to a similar share of temperature-dependent emissions of 41 %, and 64 % including heavy duty vehicles. In 2000, the overall fleet of diesel passenger cars was still small and NO_x emissions only contributed 11 % to the passenger car NO_x emissions (and 46 % for light duty vehicles), leading to a share of 9 % temperature-dependent NO_x emissions. In that case, the magnitude of the temperature correlation could only be explained when assuming temperature-dependent heavy duty vehicle NO_x emissions, which would

295 increase the share of temperature-dependent emissions to 34 %. Figure S6 of the Supplement shows that NO has decreased more strongly with temperature compared to NO_2 at all locations. NO_2 does not exhibit a temperature correlation at traffic sites. This further suggests that the temperature correlation is introduced by an emission rather than temperature-dependent chemistry, given the small share of NO_2 in primary NO_x emissions.

An additional explanation for the observed negative temperature correlation could be the influence of the planetary boundary

300 layer height (BLH). On sunny days, the BLH is driven primarily by solar radiation, which is closely related to temperature (Collaud Coen et al., 2014). A higher BLH can dilute pollutant emissions into a larger volume, which could explain the decrease of NO_x mixing ratios with temperature. While we have eliminated a major part of the BLH diurnal cycle by including only data between 9:00 and 18:00 local time (UTC+2), the day-to-day variation of the BLH remains and could contribute to the observed temperature correlation.

305 Figure 6(b) shows that O_3 is positively correlated with temperature at all sites. O_3 levels approximately double at background sites and almost triple at rural, (sub)urban and traffic sites over the observed temperature range. A close linear dependence of O_3 on temperature is observed above 15 °C at background sites (dO_3/dT = 1.8,ppbv/°C) and above 17 °C at traffic (dO_3/dT = 2.3 ppbv/°C), at (sub)urban (dO_3/dT = 3.2 ppbv/°C) and at rural sites (dO_3/dT = 2.7 ppbv/°C). A positive correlation of O_3 and temperature is expected and aligns with the current literature as discussed in Section 1. Several factors might

310 contribute to the observed O_3-temperature dependence in Switzerland including enhanced stagnation, intense solar radiation at high temperatures, enhanced reaction rates and temperature-dependent natural and anthropogenic precursor emissions. A positive correlation of BLH and temperature can introduce a positive temperature correlation for O_3 due to the intrusion of

free tropospheric air characterized by elevated O_3. At polluted sites, decreasing NO_x with temperature (6(a)) may contribute to the positive O_3-temperature relationship by alleviating titration or increasing ozone production (NO_x-saturated O_3 chemistry).

315 Background sites are not impacted by titration and do not show a NO_x-temperature dependence while still exhibiting a strong response of O_3 to temperature. This suggests that different mechanisms drive the temperature dependence of O_3 in more remote locations or that O_3 is not produced locally. Decreasing NO_x with temperature at rural sites with dominant NO_x-sensitive O_3 would lead to O_3 decreases and must therefore be counterbalanced by other processes, e.g. stagnation, solar radiation or reaction rates.

320   In Figure 6(c), we show the O_x temperature correlation, which is very similar to O_3. The major difference is an elevated baseline of O_x at low temperatures for traffic ($\sim$22 ppbv higher than for O_3 at 10°C), (sub)urban ($\sim$13 ppbv higher) and rural sites ($\sim$6 ppbv higher). This difference gets smaller with increasing temperature. The reason for this can be seen in panel (d), which shows that the share of O_3 in O_x increases with temperature. For more polluted regions as well as lower temperatures the fraction of NO_2 in O_x gets larger and vice versa. O_3 and O_x are almost equal above 25 °C at background, rural and (sub)urban

325 sites. For traffic sites the difference persists, which aligns with a remainder of 25 % NO_2 in O_x at high temperatures. This again suggests the importance of titration at traffic sites.

3.3.3   Decadal Trends of dO_3/dT and dO_x/dT

Figure 7 shows the temperature dependence of (a) O_3 (dO_3/dT) and (b) O_x (dO_x/dT) over time. dO_3/dT and dO_x/dT are calculated over the highlighted part of Figure 6(b) and (c), which shows a strong linear correlation (R^2>0.99). At all site types,

330 the temperature dependence of O_3 and O_x has decreased over time. This decrease amounts to around 1/3 and is independent of the site properties. The consistency of these decreases, considering the different O_3 trends and mechanisms of O_3 formation at the sites (as discussed in Sections 3.1 and 3.2) is remarkable. At the beginning of the century, rates ranged between 2.5 and 4 ppbv/°C, while they are between 1.5 and 2.5 ppbv/°C today. We presented the decadal trends of O_3 in Figure 3 (b), which shows decreases for background and rural sites, no significant changes for (sub)urban sites and increases for traffic sites.

335 Figure 8 highlights that these decadal trends are dependent on the temperature ranges, which we show for (a) low 10 °C ≤ T ≤ 20 °C, (b) medium 20 °C ≤ T ≤ 30 °C and (c) high T ≥ 30 °C temperatures. Background and rural sites exhibit negative O_3 trends over time for all temperature ranges, but the observed decrease gets larger with increasing temperature (e.g. for rural sites O_3 declines at 0.08 ppbv year^{-1} at low temperatures, of 0.39 ppbv year^{-1} at medium temperatures and 0.74 ppbv year^{-1} at high temperatures). For (sub)urban sites, O_3 has increased over time for low temperatures (0.10 ppbv year^{-1}), but decreased

340 for medium (-0.26 ppbv year^{-1}) and high temperatures (-0.69 ppbv year^{-1}). The trends at traffic sites are positive for low (0.29 ppbv year^{-1}), positive but insignificant for medium and negative (and insignificant) for high temperatures. This is in line with findings by Boleti et al. (2019) who reported a decline of peak O_3 (which coincides with high temperatures) at all NABEL locations, but the traffic sites, between 1990 and 2014. The rate of decadal O_3 changes is therefore highest (and positive) for polluted regions at low temperatures (and high NO_x) and lowest (and negative) for remote sites at high temperatures (and

345 low NO_x), which can explain the observed decadal decrease in dO_3/dT in Figure 7(a). O_3 levels have declined more rapidly at high versus low temperatures for background and rural sites and the trend has even reversed from positive to negative for
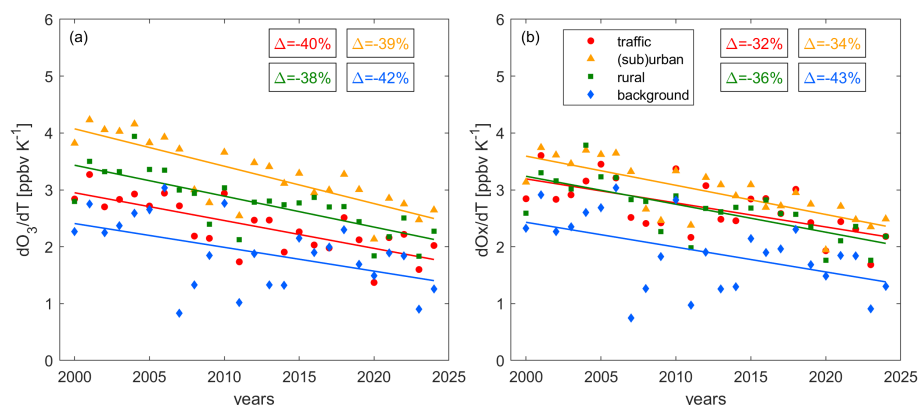
Figure 7. Changes of the (a) O_3 and (b) O_x temperature dependence over time. Data points represent the slope of O_3 and O_x vs temperature in Figure 6 (b) and (c), respectively, in the linear (highlighted) area. The chosen temperature range for the fit is 19-31 °C for traffic, (sub)urban and rural conditions and 15-27 °C for background conditions. Background sites are located at elevated altitudes and have therefore lower temperatures. Boxes show the relative change between 2000 and 2024. Solid lines denote significant (p-value ≤ 0.05) and dashed lines insignificant (p-value > 0.05) trends.
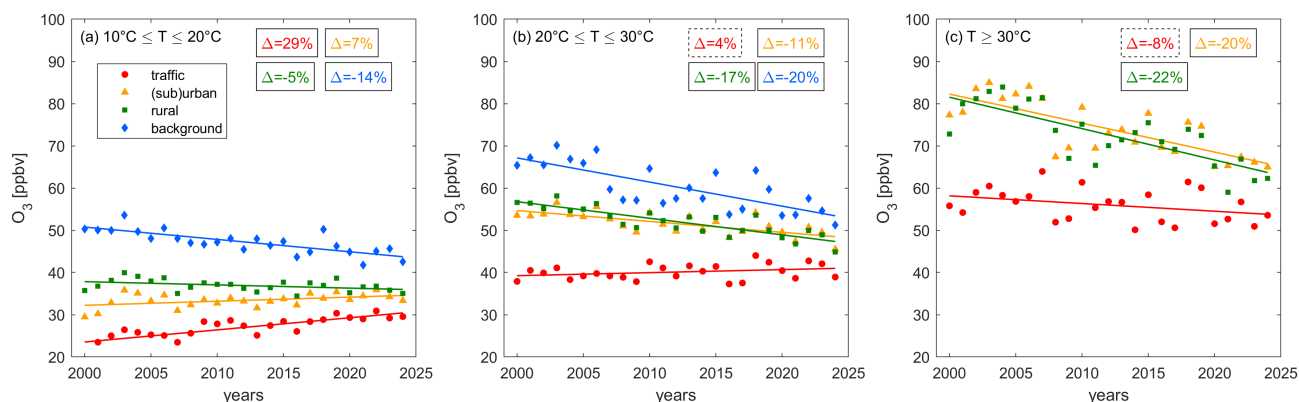

Figure 8. Decadal changes of O_3 at (a) low, (b) medium and (c) high temperatures at traffic (red), (sub)urban (orange), rural (green) and background (blue) sites. Data for high temperatures at background sites are sparse and therefore disregarded. The markers show the yearly averages and the lines represent their associated linear fits. Boxes show the relative change between 2000 and 2024. Solid lines denote significant (p-value ≤ 0.05) and dashed lines insignificant (p-value > 0.05) trends.

(sub)urban and traffic sites. Panel 7(b) highlights that the temperature dependence of O_x has decreased similarly compared to O_3 at all sites. While O_x trends for all temperature ranges are negative (Figure S7), higher temperatures show steeper declines, representing the temperature effects in decadal O_3 trends.

350   The current literature reports a similar decline in O_3 temperature sensitivity, though the underlying explanations vary. Li et al. (2025) reported a decline in the O_3 temperature dependence in the U.S. between 1990 and 2021, which they attributed

to meteorological factors, as well as increased effects of temperature-dependent BVOC emissions, dry deposition and PAN decomposition under anthropogenic NO_x reductions. A decrease in the O_3 temperature dependence with decreasing NO_x levels has additionally been reported in the U.S. among others by Wu et al. (2008) suggesting an increased NO_x loss via

355 temperature-enhanced isoprene emissions and the formation of isoprene nitrates, and isoprene ozonolysis, as well as Bloomer et al. (2009) and Rasmussen et al. (2013). Coates et al. (2016) suggested a decrease in the O_3 temperature sensitivity in response to decreases in ambient NO_x due to enhancements of reactions rates and biogenic VOCs, which was largest for high- and small for low-NO_x conditions.

Several of these studies suggest temperature-dependent VOC emissions under reductions in anthropogenic NO_x as a reason

360 for a decline in the O_3-temperature response. Under VOC-sensitive O_3 formation chemistry, temperature is known to increase O_3 levels at constant NO_x via enhanced VOCs. In turn, decreasing NO_x leads to a decline in the temperature sensitivity of O_3 when moving towards NO_x-sensitive O_3 chemistry. We find that O_3 formation in Switzerland is either dominated by the O_3 titration effect (polluted sites) or NO_x-sensitive chemistry (remote sites). Consequently, changes in VOCs are unlikely to impact O_3 formation and cannot explain the observed decline in the temperature sensitivity of O_3. Other mechanisms presented in the

365 literature, including changes in meteorology, dry deposition or PAN decomposition under NO_x reductions, could contribute to the decrease in dO_3/dT in Switzerland.

Additionally, we suggest that the share of O_3 in O_x could be a key factor in controlling the temperature-dependent trends at polluted sites (Figure 8), which directly affects the decline in O_3 temperature sensitivity (Figure 7(a)). For polluted regions with large NO_x sources and low temperatures, a considerable fraction of O_x is NO_2 (Figure 6(d)) and a decrease of NO_x over time

370 releases O_3, which affects increasing decadal trends as shown for traffic sites in Figure 8(a). At higher temperatures the share of O_3 in O_x is higher and therefore the titration effect of the decadal NO_x decline is smaller, which manifests in a less steep decadal increase for O_3 at medium temperatures (Figure 8(b)) and a further flattening at high temperatures (Figure 8(c)). NO_x reductions only become effective in reducing O_3 when the share of O_3 in O_x is large enough, which is most strongly affected by ambient NO_x levels and temperature. While this is not the case for traffic sites even at high temperatures, we observe the

375 change for (sub)urban sites, where O_3 increases over time at low temperatures. In contrast at medium temperatures, the share of O_3 in O_x is sufficiently large that the O_3 release through declining NO_x is outweighed by the reduction of O_3 formation when chemistry is NO_x-sensitive. At high temperatures, the effect of reduced O_3 formation is even larger and the decadal O_3 decline is steeper, affecting the reduction in the O_3-temperature sensitivity. We conclude that the consistent dO_3/dT trends in Switzerland are likely driven by different mechanisms, including previously suggested meteorological and chemical processes

380 at remote and background sites, with an additional role for O_3 titration at polluted sites. Further research is needed to quantify the relative role of these mechanisms in polluted and clean locations.

3.4 O_3 and O_x exceedance probabilities

Figure 9 shows the exceedance probability EP (defined as the percentage of April-August daytime hourly values above 60 ppbv) of O_3 (a) over time and (b) with temperature. The change of O_x EP with temperature can be seen in panel (c). The decadal

385 O_3 EP trend is presented in panel (a) and is similar to the O_3 trends from Figure 3(b). For rural and background sites the
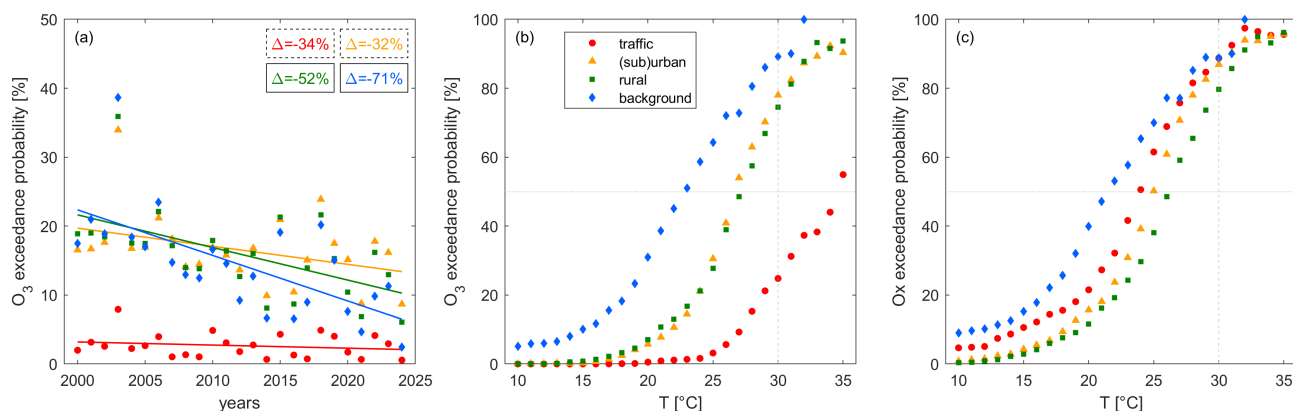
Figure 9. (a) Average decadal trends and (b) the temperature dependence of the O_3 exceedance probability and (c) the temperature dependence of the O_x exceedance probability at traffic (red), (sub)urban (orange), rural (green) and background (blue) sites. Panels (b) and (c) represent the entire study period from 2000 to 2024.

probability of O_3 exceeding the current air quality standard of 60 ppbv has decreased over time. While at the beginning of the century 20-25 % of all summertime measurements exceeded the threshold, respectively, the share has decreased to around 5-10 % today. O_3 EP at (sub)urban and traffic sites does not show a significant trend over time. The exceedance probability at (sub)urban sites is similar to rural and background sites, whereas it is much lower and only around 5 % for traffic conditions.

390 As discussed previously, this is the result of O_3 being stored in NO_2 due to titration close to NO sources. Consistent with the O_x trend shown in Figure 3(c), Figure S8 shows that O_x exceedance probabilities exhibit a significant, negative trend for all sites, highlighting NO_x-sensitive conditions under rural and background conditions and the impact of titration at traffic and (sub)urban sites (for the majority of the record).

Panel (b) shows the temperature dependence of O_3 exceedances. For low temperatures - at background sites below $2\,°C$ and
395 at the remaining sites below $15\,°C$ - O_3 exceedances do not occur. The exceedance probability then rapidly increases with temperature and above $30\,°C$, the likelihood of reaching unhealthy levels of O_3 is above 20 % at traffic sites and above 75 % at (sub)urban, rural and background sites. Figure 10 shows that these numbers have decreased by up to 35 % (percentage points) between the beginning of the century (2000-2004) and today (2020-2024), which is a positive outcome of NO_x reductions. The extent of this decrease is generally higher for higher temperatures and increasing remoteness, which is in line with our findings
400 from Figure 8 for the temperature-dependent O_3 decadal trends. Despite this effectiveness of NO_x reductions in shifting O_3 exceedances to higher temperatures, the likelihood of high-temperature days has increased 3-fold over the same time period (Figure 5(b)), weakening the described positive outcomes - a phenomenon often referred to as a climate penalty. O_x exceedance probabilities show a similar temperature dependence, as shown in panel (c). At (sub)urban, rural and background sites O_x is almost entirely O_3 and therefore the O_x and O_3 EPs are similar. For traffic sites even at high temperatures O_x still consists of
405 a significant amount of NO_2 and therefore the O_3 EP is lower than the O_x EP - at $30\,°C$ by around 50 %. With ongoing NO_x
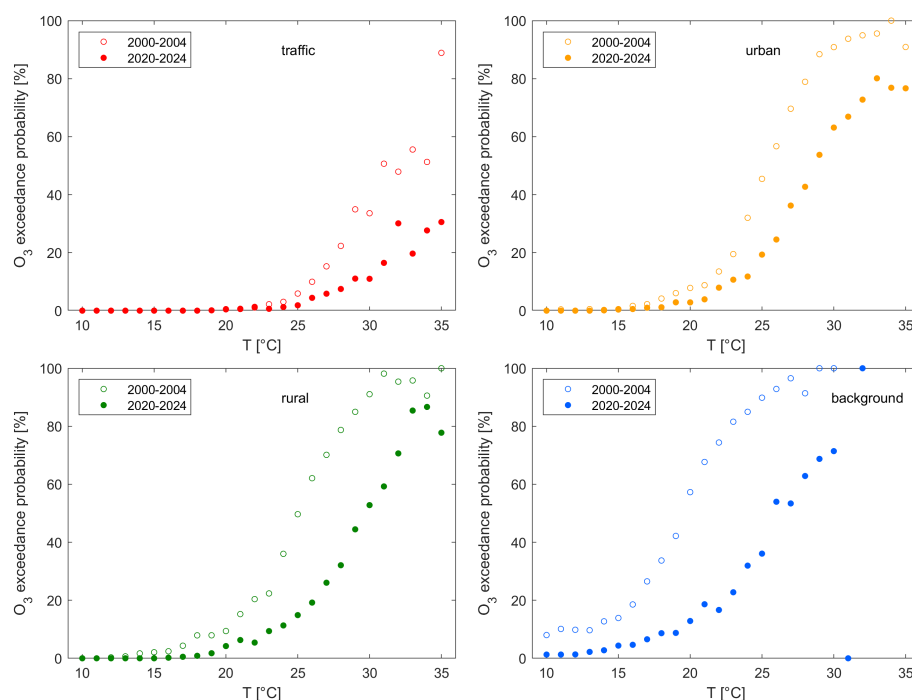
Figure 10. Temperature correlation of the O_3 exceedance probability at (a) traffic, (b) (sub)urban, (c) rural and (d) background sites as an average for the beginning of the record as open symbols (2000-2004) and today (2020-2024) as filled symbols.

reductions the EP O_3 curve will approximate the EP O_x curve when titration becomes negligible and decreases in NO_x become effective in reducing O_3.

These observations highlight the complex interplay of NO_x levels and temperature in driving the dominating O_3 chemistry in polluted environments. High temperatures are often accompanied by stagnation and high solar intensity increasing the share

410 of O_3 in O_x and thereby leading to more frequent exceedances. At the same time, these temperatures (where titration is less relevant, Figure 6(d)) create a chemical environment where NO_x reductions become effective in reducing O_3.

4   Conclusions

In this study, we have investigated the processes impacting O_3 levels under traffic, (sub)urban, rural and background conditions across Switzerland during summertime since the beginning of this century. The study is based on observations of NO, NO_2,

415 O_3 and meteorological parameters at 12 surface stations, which are part of the NABEL (Nationales Beobachtungsnetz für Luftfremdstoffe) network.

NO_x levels have continuously decreased over the past two decades at all stations, highlighting successful emission reductions. These reductions have led to O_3 decreases at rural and background stations. In contrast, average summertime O_3 has been relatively consistent at (sub)urban and even increased at traffic sites. Boleti et al. (2018) studied O_3 trends in Switzerland and

420 concluded that by 2014, average O_3 levels were decreasing at all sites. Our findings, showing the continued increase of O_3 in polluted environments beyond the study period of Boleti et al. (2018), are therefore vital and highlight the urge for continuous and stringent precursor reductions.

Using the O_3 and O_x weekend effect we show that chemistry has been dominated by NO_x-sensitive O_3 formation at background sites over the entire study period, whereas titration has been the prevailing mechanism controlling O_3 levels at traffic

425 sites. Rural sites have recently switched to NO_x-sensitive chemistry, and (sub)urban sites are currently making this shift. Despite the level of anthropogenic NO_x pollution, temperature plays an important role in controlling O_3. This strong positive correlation has several contributors, including enhanced stagnation (which often accompanies high temperatures and can lead to local O_3 build-up), increased solar radiation, the inverse temperature-correlation of NO_x and intrusion of O_3-rich free tropospheric air under a high boundary layer. We find that decadal O_3 decreases are stronger at higher temperatures or even reverse

430 from positive to negative trends at more polluted sites, which in turn, affects a continuous decrease in the temperature dependence of O_3 (dO_3/dT) over time. This observations has been previously reported by among others Wu et al. (2008), Bloomer et al. (2009), Rasmussen et al. (2013) and Li et al. (2025) in the U.S. as well as Otero et al. (2021) in Europe. While the reason for this observation is regionally different and not fully understood up to this point, we offer an explanation related to the share of O_3 in O_x titration for polluted sites, which is smallest for low temperatures and polluted sites and increases with rising

435 temperature and increasing remoteness. While we find a similar decrease in O_3-temperature sensitivity at all sites, the effect of titration is largest at most polluted sites and other processes likely dominate the trend at more remote locations.

The exceendance probabilities for O_3 and O_x of the current O_3 Swiss air quality standard additionally show a strong temperature dependence and unhealthy levels occur with a probability of more than 80 % at (sub)urban, rural and background sites on hot summer days (T ≥ 30 °C). Due to NO_x reductions, the occurrence of O_3 exceedances is now limited to the highest temper-

440 atures, however, the share of summer days exceeding 30 °C is around 3 times larger today than it was at the beginning of the century, which offsets part of the success in emission reductions. O_3 levels at traffic sites are still suppressed by large amounts of NO_x and we expect increases in O_3 exceedances, particularly at lower temperatures, for the coming years before the impact of titrations becomes negligible and NO_x reductions effective. Many different factors, including the rate of NO_x reductions and meteorological parameters, make it challenging to predict the crossover point. Assuming a change from dominant titration

445 to dominant NO_x-sensitive O_3 formation for rural sites in the middle of the studied period and for (sub)urban sites in recent years, the crossover occurs when O_3 makes up at least 85 % of O_x. If we assume a continued increase in the share of O_3 in O_x of 1 % year^{-1} (Figure 3(d)), chemistry at traffic sites would be dominated by NO_x-sensitive O_3 formation rather than titration starting in 2035. Aksoyoglu et al. (2014) reported the dominant effect of titration on O_3 levels in Switzerland between 1990 and 2005. Twenty years later, polluted sites are still titration-dominated despite strong precursor emission declines, highlighting

450 the challenge of sufficient pollutant reductions to achieve clean air.

These findings emphasize that O_3 remains an air quality concern in Switzerland. NO_x reductions are now effective in reducing O_3 levels at (sub)urban, rural and background sites, but exceedances, particularly at high temperatures, remain frequent. Therefore, rapid NO_x reductions are required to reduce O_3 levels, which are also needed to overcome the dominance of titration at polluted sites. Continued long-term monitoring of O_3 and its precursors is critical to identify changes in the non-linear

455   processes, which drive the abundance of O_3 and impact local air quality. Of particular benefit in Switzerland would be the addition of long-term speciated VOC measurements at multiple sites, which are currently strongly limited, but are important precursors to local O_3 formation and can support our understanding of the shifting role of natural and anthropogenic precursors. Finally, more research is needed to understand and monitor the climate penalty on O_3 under continuous anthropogenic precursor reductions and increasing temperatures.

460   *Data availability.* Trace gas measurements and meteorological observations used in this study can be obtained from the data query tool of the Federal Office of the Environment (2025) (in German: Bundesamt für Umwelt BAFU): https://www.bafu.admin.ch/bafu/en/home/topics/air/luft belastung/data/data-query-nabel.html

References

470   Adame, J., Gutiérrez-Álvarez, I., Cristofanelli, P., Notario, A., Bogeat, J., López, A., Gómez, A., Bolívar, J., and Yela, M.: Surface ozone trends over a 21-year period at El Arenosillo observatory (Southwestern Europe), Atmospheric Research, 269, 106 048, https://doi.org/10.1016/j.atmosres.2022.106048, 2022.

Aksoyoglu, S., Keller, J., Ciarelli, G., Prévôt, A. S., and Baltensperger, U.: A model study on changes of European and Swiss particulate matter, ozone and nitrogen deposition between 1990 and 2020 due to the revised Gothenburg protocol, Atmospheric Chemistry and

475   Physics, 14, 13 081–13 095, https://doi.org/10.5194/acp-14-13081-2014, 2014.

Baidar, S., Hardesty, R., Kim, S.-W., Langford, A., Oetjen, H., Senff, C., Trainer, M., and Volkamer, R.: Weakening of the weekend ozone effect over California's South Coast Air Basin, Geophysical Research Letters, 42, 9457–9464, https://doi.org/10.1002/2015GL066419, 2015.

Black, E., Blackburn, M., Harrison, G., Hoskins, B., and Methven, J.: Factors contributing to the summer 2003 European heatwave, Weather,

480   59, 217–223, https://doi.org/10.1256/wea.74.04, 2004.

Bloomer, B. J., Stehr, J. W., Piety, C. A., Salawitch, R. J., and Dickerson, R. R.: Observed relationships of ozone air pollution with temperature and emissions, Geophysical research letters, 36, https://doi.org/10.1029/2009GL037308, 2009.

Boleti, E., Hüglin, C., and Takahama, S.: Ozone time scale decomposition and trend assessment from surface observations in Switzerland, Atmospheric Environment, 191, 440–451, https://doi.org/10.1016/j.atmosenv.2018.07.039, 2018.

485   Boleti, E., Hüglin, C., and Takahama, S.: Trends of surface maximum ozone concentrations in Switzerland based on meteorological adjustment for the period 1990–2014, Atmospheric environment, 213, 326–336, https://doi.org/10.1016/j.atmosenv.2019.05.018, 2019.

Boleti, E., Hüglin, C., Grange, S. K., Prévôt, A. S., and Takahama, S.: Temporal and spatial analysis of ozone concentrations in Europe based on timescale decomposition and a multi-clustering approach, Atmospheric Chemistry and Physics, 20, 9051–9066, https://doi.org/10.5194/acp-20-9051-2020, 2020.

490   Chang, K.-L., McDonald, B. C., Harkins, C., and Cooper, O. R.: Surface ozone trend variability across the United States and the impact of heat waves (1990–2023), Atmospheric Chemistry and Physics, 25, 5101–5132, https://doi.org/10.5194/acp-25-5101-2025, 2025.

Chinkin, L. R., Coe, D. L., Funk, T. H., Hafner, H. R., Roberts, P. T., Ryan, P. A., and Lawson, D. R.: Weekday versus weekend activity patterns for ozone precursor emissions in California's South Coast Air Basin, Journal of the Air & Waste Management Association, 53, 829–843, https://doi.org/10.1080/10473289.2003.10466223, 2003.

495   Coates, J., Mar, K. A., Ojha, N., and Butler, T. M.: The influence of temperature on ozone production under varying NO x conditions–a modelling study, Atmospheric Chemistry and Physics, 16, 11 601–11 615, https://doi.org/10.5194/acp-16-11601-2016, 2016.

Collaud Coen, M., Praz, C., Haefele, A., Ruffieux, D., Kaufmann, P., and Calpini, B.: Determination and climatology of the planetary boundary layer height above the Swiss plateau by in situ and remote sensing measurements as well as by the COSMO-2 model, Atmospheric Chemistry and Physics, 14, 13 205–13 221, https://doi.org/10.5194/acp-14-13205-2014, 2014.

500   Cooper, O., Derwent, D., Collins, B., Doherty, R., Stevenson, D., Stohl, A., and Hess, P.: Chapter 1: Conceptual Overview of Hemispheric or Intercontinental Transport of Ozone and Particulate Matter, in: Hemispheric transport of air pollution 2010: Part A-Tropospheric ozone and particulate matter, edited by DENTENER, F., KEATING, T. J., and AKIMOTO, H., United Nations, New York and Geneva, 2011.

Crutzen, P. J.: Tropospheric ozone: An overview, Springer, https://doi.org/10.1007/978-94-009-2913-5_1, 1988.

Denman, K. L., Brasseur, G., Chidthaisong, A., Ciais, P., Cox, P. M. M., Dickinson, R. E. E., Hauglustaine, D., Heinze, C., Holland, E.,

505   Jacob, D., Lohmann, U., Ramachandran, S., da Silva Dias, P. L., Wofsy, S. C. C., Zhang, X., Arora, V., Baker, D., Bonan, G., Bousquet, P.,

21

Canadell, J., Christian, J., Clark, D., Dameris, M., Dentener, F., Easterling, D., Eyring, V., Feichter, J., Friedlingstein, P., Fung, I., Fuzzi, S., Gong, S., Gruber, N., Guenther, A., Gurney, K., Henderson-Sellers, A., House, J., Jones, A., Jones, C., Kärcher, B., Kawamiya, M., Lassey, K., Le Quéré, C., Leck, C., Lee-Taylor, J., Malhi, Y., Masarie, K., Mcfiggans, G., Menon, S., Miller, J., Peylin, P., Pitman, A., Quaas, J., Raupach, M., Rayner, P., Rehder, G., Riebesell, U., Rödenbeck, C., Rotstayn, L., Roulet, N., Sabine, C., Schultz, M., Schulz, M., Schwartz, S., Steffen, W., Stevenson, D., Tian, Y., Trenberth, K., Van Noije, T., Wild, O., Zhang, T., and Zhou, L.: Couplings between changes in the climate system and biogeochemistry, Climate Change 2007: The Physical Science Basis. Contribution of Working Group I to the Fourth Assessment Report of the Intergovernmental Panel on Climate Change The Physical Science Basis, pp. 499–587, 2007.

Derwent, R. G., Utembe, S. R., Jenkin, M. E., and Shallcross, D. E.: Tropospheric ozone production regions and the intercontinental origins of surface ozone over Europe, Atmospheric Environment, 112, 216–224, https://doi.org/10.1016/j.atmosenv.2015.04.049, 2015.

Dong, B., Sutton, R. T., and Shaffrey, L.: Understanding the rapid summer warming and changes in temperature extremes since the mid-1990s over Western Europe, Climate Dynamics, 48, 1537–1554, https://doi.org/10.1007/s00382-016-3158-8, 2017.

Empa: Luftschadstoff-Emissionen des Strassenverkehrs 1990–2060, Report, Bern, Switzerland, available from: https://www.bafu.admin.ch/bafu/de/home/themen/luft/publikationen-studien/publikationen/luftschadstoff-emissionen-des-strassenverkehrs-1990-2060.html, 2024.

Empa and BAFU: Technischer Bericht zum Nationalen Beobachtungsnetz für Luftfremdstoffe (NABEL) 2024, Technical report, Dübendorf, Switzerland, available from: https://www.bafu.admin.ch/bafu/de/home/themen/luft/zustand/daten/nationales-beobachtungsnetz-fuer-luftfremdstoffe--nabel-/berichte-des-nabel.html, 2024.

European Environmental Agency: Harm to human health from air pollution in Europe: burden of disease status, https://doi.org/10.2800/3950756, "accessed on 2025-01-09", 2024.

Federal Office of the Environment: Data query NABEL, https://www.bafu.admin.ch/bafu/en/home/topics/air/luftbelastung/data/data-query-nabel.html, [Dataset], 2025.

Federal Office of Topography swisstopo: swissBOUNDARIES3D, available from: https://www.swisstopo.admin.ch/en/landscape-model-swissboundaries3dAdditional-information, 2024.

Fujita, E. M., Stockwell, W. R., Campbell, D. E., Keislar, R. E., and Lawson, D. R.: Evolution of the magnitude and spatial extent of the weekend ozone effect in California's South Coast Air Basin, 1981–2000, Journal of the Air & Waste Management Association, 53, 802–815, https://doi.org/10.1080/10473289.2003.10466225, 2003.

Geddes, J. A., Murphy, J. G., and Wang, D. K.: Long term changes in nitrogen oxides and volatile organic compounds in Toronto and the challenges facing local ozone control, Atmospheric Environment, 43, 3407–3415, https://doi.org/10.1016/j.atmosenv.2009.03.053, 2009.

Grange, S. K., Lewis, A. C., Moller, S. J., and Carslaw, D. C.: Lower vehicular primary emissions of NO2 in Europe than assumed in policy projections, Nature Geoscience, 10, 914–918, https://doi.org/10.1038/s41561-017-0009-0, 2017.

Grange, S. K., Farren, N. J., Vaughan, A. R., Rose, R. A., and Carslaw, D. C.: Strong temperature dependence for light-duty diesel vehicle NO x emissions, Environmental Science & Technology, 53, 6587–6596, https://doi.org/10.1021/acs.est.9b01024, 2019.

Grange, S. K., Farren, N. J., Vaughan, A. R., Davison, J., and Carslaw, D. C.: Post-dieselgate: evidence of NOx emission reductions using on-road remote sensing, Environmental science & technology letters, 7, 382–387, https://doi.org/10.1021/acs.estlett.0c00188, 2020.

Guenther, A., Jiang, X., Heald, C. L., Sakulyanontvittaya, T., Duhl, T. a., Emmons, L., and Wang, X.: The Model of Emissions of Gases and Aerosols from Nature version 2.1 (MEGAN2. 1): an extended and updated framework for modeling biogenic emissions, Geoscientific Model Development, 5, 1471–1492, https://doi.org/10.5194/gmd-5-1471-2012, 2012.

Huang, T., Zhu, X., Zhong, Q., Yun, X., Meng, W., Li, B., Ma, J., Zeng, E. Y., and Tao, S.: Spatial and temporal trends in global emissions of nitrogen oxides from 1960 to 2014, Environmental science & technology, 51, 7992–8000, https://doi.org/10.1021/acs.est.7b02235, 2017.

545 Hüglin, C. and Rohrbach, S.: Zeitliche Entwicklung der NO2 – Immissionen an verkehrs- belasteten städtischen Standorten, Technical report, Dübendorf, Switzerland, available from: https://www.empa.ch/documents/56101/29574162/Trend+NO2+Immissionen+Stadt+2022.pdf/ddba8b88-c599-4ed4-8b94- cc24670be683?version=1.0t=1717509377000download=true, 2022.

Hüglin, C., Buchmann, B., Steinbacher, M., and Emmenegger, L.: The Swiss National Air Pollution Monitoring Network (NABEL)–Bridging
550 Science and Environmental Policy, Chimia, 78, 722–727, https://doi.org/10.2533/chimia.2024.722, 2024.

Levitt, S. B. and Chock, D. P.: Weekday-weekend pollutant studies of the Los Angeles basin, Journal of the Air Pollution Control Association, 26, 1091–1092, https://doi.org/10.1080/00022470.1976.10470368, 1976.

Li, S., Wang, H., and Lu, X.: Anthropogenic emission controls reduce summertime ozone–temperature sensitivity in the United States, Atmospheric Chemistry and Physics, 25, 2725–2743, https://doi.org/10.5194/acp-25-2725-2025, 2025.

555 Massagué, J., Torre-Pascual, E., Carnerero, C., Escudero, M., Alastuey, A., Pandolfi, M., Querol, X., and Gangoiti, G.: Extreme ozone episodes in a major Mediterranean urban area, Atmospheric Chemistry and Physics, 24, 4827–4850, https://doi.org/10.5194/acp-24-4827- 2024, 2024.

McDonald, B. C., De Gouw, J. A., Gilman, J. B., Jathar, S. H., Akherati, A., Cappa, C. D., Jimenez, J. L., Lee-Taylor, J., Hayes, P. L., McKeen, S. A., et al.: Volatile chemical products emerging as largest petrochemical source of urban organic emissions, Science, 359,
560 760–764, https://doi.org/10.1126/science.aaq0524, 2018.

McDuffie, E. E., Smith, S. J., O'Rourke, P., Tibrewal, K., Venkataraman, C., Marais, E. A., Zheng, B., Crippa, M., Brauer, M., and Martin, R. V.: A global anthropogenic emission inventory of atmospheric pollutants from sector-and fuel-specific sources (1970–2017): an applica- tion of the Community Emissions Data System (CEDS), Earth System Science Data Discussions, 2020, 1–49, https://doi.org/10.5194/essd- 12-3413-2020, 2020.

565 Murphy, J. G., Day, D. A., Cleary, P. A., Wooldridge, P. J., Millet, D. B., Goldstein, A. H., and Cohen, R. C.: The weekend effect within and downwind of Sacramento–Part 1: Observations of ozone, nitrogen oxides, and VOC reactivity, Atmospheric Chemistry and Physics, 7, 5327–5339, https://doi.org/10.5194/acp-7-5327-2007, 2007.

Nault, B., Laughner, J., Wooldridge, P., Crounse, J., Dibb, J., Diskin, G., Peischl, J., Podolske, J., Pollack, I., Ryerson, T., et al.: Lightning NOx emissions: Reconciling measured and modeled estimates with updated NOx chemistry, Geophysical Research Letters, 44, 9479–
570 9488, https://doi.org/10.1002/2017GL074436, 2017.

Nussbaumer, C. M. and Cohen, R. C.: The role of temperature and NO x in ozone trends in the Los Angeles Basin, Environmental Science & Technology, 54, 15 652–15 659, https://doi.org/10.1021/acs.est.0c04910, 2020.

Nuvolone, D., Petri, D., and Voller, F.: The effects of ozone on human health, Environmental Science and Pollution Research, 25, 8074–8088, https://doi.org/10.1007/s11356-017-9239-3, 2018.

575 Oikawa, P., Ge, C., Wang, J., Eberwein, J., Liang, L., Allsman, L., Grantz, D., and Jenerette, G.: Unusually high soil nitrogen oxide emissions influence air quality in a high-temperature agricultural region, Nature communications, 6, 8753, https://doi.org/10.1038/ncomms9753, 2015.

Ordoñez, C., Mathis, H., Furger, M., Henne, S., Hüglin, C., Staehelin, J., and Prévôt, A. S.: Changes of daily surface ozone maxima in Switzerland in all seasons from 1992 to 2002 and discussion of summer 2003, Atmospheric chemistry and physics, 5, 1187–1203,
580 https://doi.org/10.5194/acp-5-1187-2005, 2005.

Otero, N., Rust, H. W., and Butler, T.: Temperature dependence of tropospheric ozone under NOx reductions over Germany, Atmospheric Environment, 253, 118 334, https://doi.org/10.1016/j.atmosenv.2021.118334, 2021.

Perdigones, B. C., Lee, S., Cohen, R. C., Park, J.-H., and Min, K.-E.: Two decades of changes in summertime ozone production in California's South Coast Air Basin, Environmental Science & Technology, 56, 10 586–10 595, https://doi.org/10.1021/acs.est.2c01026, 2022.

Pollack, I., Ryerson, T., Trainer, M., Parrish, D., Andrews, A., Atlas, E. L., Blake, D., Brown, S., Commane, R., Daube, B., et al.: Airborne and ground-based observations of a weekend effect in ozone, precursors, and oxidation products in the California South Coast Air Basin, Journal of Geophysical Research: Atmospheres, 117, https://doi.org/10.1029/2011JD016772, 2012.

Porter, W. C. and Heald, C. L.: The mechanisms and meteorological drivers of the summertime ozone–temperature relationship, Atmospheric Chemistry and Physics, 19, 13 367–13 381, https://doi.org/10.5194/acp-19-13367-2019, 2019.

Pusede, S. and Cohen, R.: On the observed response of ozone to NOx and VOC reactivity reductions in San Joaquin Valley California 1995–present, Atmospheric Chemistry and Physics, 12, 8323–8339, https://doi.org/10.5194/acp-12-8323-2012, 2012.

Pusede, S. E., Steiner, A. L., and Cohen, R. C.: Temperature and recent trends in the chemistry of continental surface ozone, Chemical reviews, 115, 3898–3918, https://doi.org/10.1021/cr5006815, 2015.

Qin, M., She, Y., Wang, M., Wang, H., Chang, Y., Tan, Z., An, J., Huang, J., Yuan, Z., Lu, J., et al.: Increased urban ozone in heatwaves due to temperature-induced emissions of anthropogenic volatile organic compounds, Nature Geoscience, 18, 50–56, https://doi.org/10.1038/s41561-024-01608-w, 2025.

Rasmussen, D., Hu, J., Mahmud, A., and Kleeman, M. J.: The ozone–climate penalty: past, present, and future, Environmental science & technology, 47, 14 258–14 266, https://doi.org/10.1021/es403446m, 2013.

Schär, C., Vidale, P. L., Lüthi, D., Frei, C., Häberli, C., Liniger, M. A., and Appenzeller, C.: The role of increasing temperature variability in European summer heatwaves, Nature, 427, 332–336, https://doi.org/10.1038/nature02300, 2004.

Schweizerischer Bundesrat: 814.318.142.1 Luftreinhalte-Verordnung, https://www.fedlex.admin.ch/eli/cc/1986/208_208_208/de#app7ahref0, 1985.

Seinfeld, J. H. and Pandis, S. N.: Atmospheric chemistry and physics: from air pollution to climate change, John Wiley & Sons, 2016.

Sindelarova, K., Granier, C., Bouarar, I., Guenther, A., Tilmes, S., Stavrakou, T., Müller, J.-F., Kuhn, U., Stefani, P., and Knorr, W.: Global data set of biogenic VOC emissions calculated by the MEGAN model over the last 30 years, Atmospheric Chemistry and Physics, 14, 9317–9341, https://doi.org/10.5194/acp-14-9317-2014, 2014.

Twardosz, R., Walanus, A., and Guzik, I.: Warming in Europe: recent trends in annual and seasonal temperatures, Pure and Applied Geophysics, 178, 4021–4032, https://doi.org/10.1007/s00024-021-02860-6, 2021.

Wang, Y., van Pinxteren, D., Tilgner, A., Hoffmann, E. H., Hell, M., Bastian, S., and Herrmann, H.: Ozone (O3) observations in Saxony, Germany, for 1997–2020: trends, modelling and implications for O3 control, Atmospheric Chemistry and Physics, 25, 8907–8927, https://doi.org/10.5194/acp-25-8907-2025, 2025a.

Wang, Y., Yang, Y., Yuan, Q., Li, T., Zhou, Y., Zong, L., Wang, M., Xie, Z., Ho, H. C., Gao, M., Tong, S., Lolli, S., and Zhang, L.: Substantially underestimated global health risks of current ozone pollution, Nature Communications, 16, 102, https://doi.org/10.1038/s41467-024-55450-0, 2025b.

Weng, H., Lin, J., Martin, R., Millet, D. B., Jaeglé, L., Ridley, D., Keller, C., Li, C., Du, M., and Meng, J.: Global high-resolution emissions of soil NOx, sea salt aerosols, and biogenic volatile organic compounds, Scientific Data, 7, 148, https://doi.org/10.1038/s41597-020-0488-5, 2020.

Wu, S., Mickley, L. J., Leibensperger, E. M., Jacob, D. J., Rind, D., and Streets, D. G.: Effects of 2000–2050 global change on ozone air quality in the United States, Journal of Geophysical Research: Atmospheres, 113, https://doi.org/10.1029/2007JD008917, 2008.

620   Wu, W., Fu, T.-M., Arnold, S. R., Spracklen, D. V., Zhang, A., Tao, W., Wang, X., Hou, Y., Mo, J., Chen, J., Li, Y., Feng, X., Lin, H., Huang, Z., Zheng, J., Shen, H., Zhu, L., Wang, C., Ye, J., and Yang, X.: Temperature-dependent evaporative anthropogenic VOC emissions significantly exacerbate regional ozone pollution, Environmental Science & Technology, 58, 5430–5441, https://doi.org/10.1021/acs.est.3c09122, 2024.

Yan, Y., Pozzer, A., Ojha, N., Lin, J., and Lelieveld, J.: Analysis of European ozone trends in the period 1995–2014, Atmospheric Chemistry
625   and Physics, 18, 5589–5605, https://doi.org/10.5194/acp-18-5589-2018, 2018.